JOURNAL OF APPLIED ELECTROCHEMISTRY 12 (1982) 281–290

Anodic reactions of Ni_3S_2, β-NiS and nickel matte

D. C. PRICE*, W. G. DAVENPORT†

Department of Mining and Metallurgical Engineering, McGill University, Montreal, Quebec, Canada

Received 31 July 1981

The anodic reactions of Ni_3S_2, β-NiS and a commercial nickel matte have been investigated galvanostatically. It is shown that the matte as well as both compounds decompose with loss of nickel ions through the series of phases: $Ni_{1.5}S_2 \rightarrow Ni_{1.2}S_2 \rightarrow NiS_2 \rightarrow Ni^{2+} + 2S^0$

1. Introduction

Modern interest in the direct electrorefining of nickel matte began with the work of Loshkarev *et al.* [1] in 1945. This later led to the INCO matte electrolysis process [2, 3] performed at Thompson, Manitoba, and similar processes which are now in operation at the Norlisk Mining and Metallurgical Combine, USSR, and the Shimura Nickel Company in Tokyo, Japan [4].

Since 1945 much work has been done to elucidate the exact nature of the leaching reactions, usually by the measurement of static or dynamic potentials, often coupled with solid state analysis. A comprehensive review of the literature will not be presented in this work, both because summaries and reviews of previous work are available [5–11], and because the analysis now presented is apparently novel to this system.

The present investigation involves the anodic treatment of synthetic Ni_3S_2 and β-NiS, and samples of a commercial nickel matte (kindly supplied by the International Nickel Company Limited) under constant current conditions. The results are analysed by methods based on classical chronopotentiometric theory.

2. Experimental equipment and materials

2.1. *Experimental apparatus*

All the experiments were performed under galvanostatic conditions in an unpartitioned cell in a thermostatically controlled water bath. During anodic treatment, the potential at the specimen surface was measured relative to a standard calomel electrode via a Luggin probe and was continuously plotted on a chart recorder.

2.2. *Mineral and matte specimens*

2.2.1. Ni_3S_2 and β-NiS. Heazlewoodite Ni_3S_2, and millerite, β-NiS, were synthesized from spectrographically pure elements in a two-bulb system, previously described for the synthesis of copper sulphides [12]. These minerals were melted, cast in the synthesis tubes and then sectioned to give discs of material 3–6 mm thick. Optical analysis indicated that a single phase was present in each synthesis and X-ray diffraction analysis confirmed that the phase was either heazlewoodite or millerite.

2.2.2. Nickel matte. An INCO 'baby' matte anode was sectioned into cubes with edges of approximately 1 cm. (Analyses of a number of specimens indicated that the matte composition was: nickel 74%, copper 3%, cobalt 0.7%, sulphur 20%.) Optical analysis indicated the presence of two phases in the matte. X-ray diffraction analyses showed that these phases were heazlewoodite and nickel metal.

Electrical contact to each specimen was made by a copper wire attached to one surface of the specimen with a conductive epoxy resin. The specimen was then mounted in a low temperature

*Present address: Duval Corporation, 4715 East Fort Lowell Road, Tucson, Arizona 85712, USA.
†Present address: Department of Metallurgy, University of Arizona, Tucson, Arizona 87521, USA.

0021–891X/82/030281–10$03.70/0

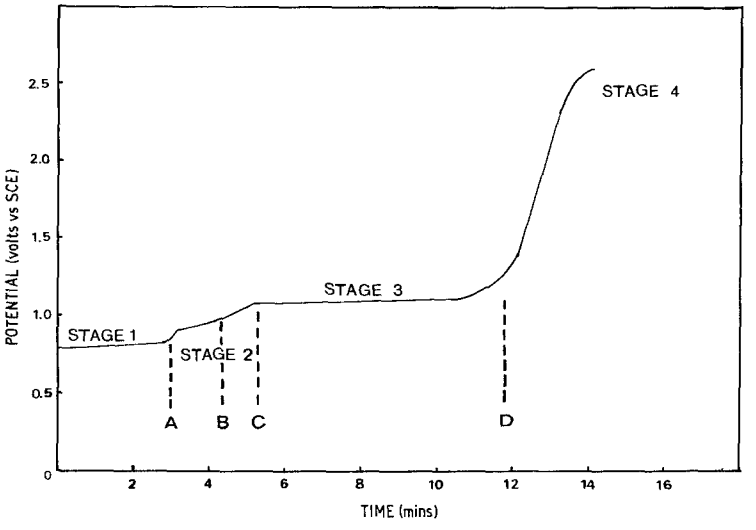

Fig. 1. Potential–time relationship for Ni_3S_2 anodically treated in 100 g H_2SO_4 dm^{-3}, 750 Am^{-2}, 50° C.

epoxy resin such that only the face opposite the wire connection was exposed. The area of the exposed face was determined photographically.

3. Results and analysis

3.1. Ni_3S_2

The anodic treatment of specimens of synthetic Ni_3S_2 was performed at 50° C in a solution of 100 g H_2SO_4 dm^{-3} at current densities of 100 to 2500 Am^{-2}.

The form of the potential–time plot in all cases was essentially as illustrated in Fig. 1, which can be conveniently described in terms of four stages. In Stage 1 the potential increased very slowly, but at the end of Stage 1, point A, a rapid transition occurred to a slightly higher potential which was the beginning of Stage 2. During Stage 2, the potential rose at a greater rate than in Stage 1 and passed through a point of inflection (point B) before the rate of potential increase began to decrease at the start of Stage 3 (point C), Stage 3 again consisted of a slowly increasing potential until a further potential increase occurred at a point D to a high and slightly varying potential.

Solution and solid phase analyses demonstrated that nickel was preferentially leached from the sulphide during Stages 1 and 2 indicating a reaction of the form:

$$Ni_3S_2 \rightarrow Ni_{3-x}S_2 + xNi^{2+} + 2xe^- . \quad (1)$$

During Stage 3 sulphur was also detected, formed by the reaction:

$$Ni_{3-x}S_2 \rightarrow (3-x)Ni^{2+} + 2S^0 + 2(3-x)e^- . \quad (2)$$

During Stage 4 oxygen was found to be evolved in addition to mineral dissolution.

The values of $i_o t^{1/2}$ have been calculated and the average of the values for each current density are listed in Table 1. It can be seen, within the limits of experimental error, that

$$i_o t^{1/2} = \text{constant} \quad (3)$$

for all stages.

In previous papers [13, 14], it was shown that the solid electrode system, i.e. the mineral crystal structure, can be considered analogous to an unstirred convection free solution, and hence the classic equations of chronopotentiometry can be applied to the diffusion of the mobile nickel ions through the crystal.

By comparison with chronopotentiometric theory [15], for a diffusion controlled step-wise reaction where the product of the first stage becomes the reactant in the second stage (cf. Equations 1 and 2) [16]:

$$\frac{n_2}{n_1} = \frac{(t_1 + t_2)^{1/2} - t_1^{1/2}}{t_1^{1/2}} \quad (4)$$

where: n_1 and n_2 are the number of electron equivalents involved in the electrolysis of 1 mole of the electroactive species in Stage 1 and Stage 2,

Table 1. The anodic treatment of Ni_3S_2. Average values of $i_o t^{1/2}$ Am^{-2} $s^{1/2}$

	$i_o t^{1/2}$			
Current density (Am^{-2})	*Stage 1*	*Inflection*	*Stages (1 + 2)*	*Stages (1 + 2 + 3)*
(1) Present investigation 50° C, 100 g H_2SO_4 dm^{-3}				
100	10 218	–	–	–
250	9 995	12 514	13 693	–
500	9 967	13 211	14 946	21 960
750	10 884	13 139	14 711	21 945
1 000	11 061	12 208	12 845	20 235
1 250	11 195	12 853	13 874	21 025
1 500	10 457	12 187	13 972	20 751
2 000	11 477	14 319	16 135	23 379
2 500	10 781	12 399	14 555	21 078
All values	10 726 ±1 000	12 853 ±1 240	14 353 ±1 321	21 651 ±1 776
(2) Kato and Oki [17] 40° C, 1 mole dm^{-3} H_2SO_4 + 0.1 mol dm^{-3} $NiSO_4$				
Extrapolated to $t^{1/2} = 0$			12 609	19 083

respectively; t_1 and t_2 are the respective transaction times for Stage 1 and Stage 2. From Equations 1 and 2:

$$\frac{n_2}{n_1} = \frac{3-x}{x} \tag{5}$$

i.e. the value of x can be found from measurements of the transition times.

In the present case, nickel was found to dissolve preferentially to the end of Stage (1 + 2), i.e. point C in Fig. 1, and hence t_1 may have the values denoted by points A, B or C; t_2 will be given from point D.

From the values of t_1, t_2 and i_o and Equations 4 and 5, the values of x have been calculated. The results indicate that N_3S_2 decomposes in stages represented by the scheme:

$$Ni_3S_2 \rightarrow Ni_{1.5(\pm 0.1)}S_2 \rightarrow Ni_{1.2(\pm 0.1)}S_2 \rightarrow Ni_{1.0(\pm 0.1)}S_2. \tag{6}$$

It appears likely that the two well-defined potential increases correspond to the compounds Ni_3S_4 and NiS_2. The point of inflection at $Ni_{1.2}S_2$ may indicate that this is an unusually stable phase or a true compound.

X-ray analysis of the residues indicated the presence of β-NiS and sulphur in addition to Ni_3S_2, although the first compound is not predicted by chronopotentiometric analysis. However, these X-ray results may be due to alterations in the phases after the current has been removed, or may be due to the similarity in the X-ray patterns of β-NiS and a phase with less nickel than represented by this formula. The latter would be in agreement with the work of Kato and Oki [17] where the nickel content of the surface material was shown to be less than 60% (cf. NiS–65% Ni, Ni_3S_4–58% Ni) although the phase was identified as β-NiS by X-ray diffraction. Similar results have previously been shown in the anodic treatment of bornite [13] Cu_5FeS_4, where X-ray diffraction indicated the presence of the compound Cu_3FeS_4 but electron probe microanalysis proved that this compound was $Cu_{2.5}FeS_4$.

The re-analysis of the transition time measurements of Kato and Oki [17] results in the reaction scheme:

$$Ni_3S_2 \rightarrow NiS_2 \rightarrow Ni^{2+} + S^0. \tag{7}$$

Their anodic treatments were performed at 40° C in a solution of 1 mol dm^{-3} H_2SO_4 + 0.1 mol dm^{-3} $NiSO_4$. The analysis of their results is different to that performed for the results of the present investigation because their $i_o t^{1/2}$ products for the two reported transitions are not constant but vary with time as shown in Fig. 2.

From classical chronopotentiometric theory, extrapolation of $i_o t^{1/2}$ versus i_o to $i_o = 0$ will give the value of $i_o t^{1/2}$ for diffusion control. However, it has been shown previously [14] for the anodic dissolution of the simple copper sulphides that the data are best represented by an equation of the form:

$$i_o t^{1/2} = K - i_x t^{1/2} \tag{8}$$

where K is the value of $i_o t^{1/2}$ at $t^{1/2} = 0$ and i_x is a constant. The same argument can be applied to both stages of the reaction, and for the second stage the intersection at $t^{1/2} = 0$ will correspond to $i_o[(t_1 + t_2) - t_1]^{1/2}$ for diffusion control. Hence, from these two values and Equations 4 and 5, the composition of the intermediate phase can be calculated.

The $i_o t^{1/2}$ values for diffusion control calculated from Fig. 2 are listed in Table 1 and the composition of the intermediate phase calculated

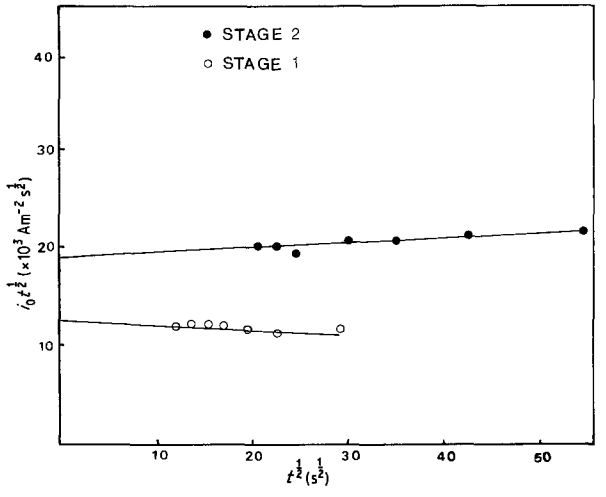

Fig. 2. $i_0 t^{1/2}$ versus $t^{1/2}$ relationship for Ni_3S_2 treatment. Recalculated from the work of Kato and Oki [17]. 40° C, 1 mol dm^{-3} H_2SO_4 + 0.1 mol dm^{-3} $NiSO_4$.

from these values is $Ni_{1.0 \pm 0.2}S_2$, in agreement with the experimental results of the present investigation.

Equation 8 indicates that $i_0 t^{1/2}$ will decrease with an increase of $t^{1/2}$, but it can be seen in Fig. 2 that $i_0 t^{1/2}$ for the second stage increases with an increase of $t^{1/2}$. In the previous application of this form of Equation 14 it was postulated that i_x is a measure of the chemical dissolution effect of the solution. It has not, however, been possible to experimentally confirm the effects of various solutions of Ni_3S_2 or the intermediates in the present investigation. It has been shown that this analysis gives consistent results and that they are nevertheless in agreement with the previous work of DeRantny and Breckpot [18]. In the investigation of these workers, it was indicated that the conversion of NiS to NiS_2 can be anticipated from the position of the metal ions in the NiS structure. However, the present results do not agree with their findings that the composition may approach $Ni_{0.6}S_2$ before sulpur is formed.

Chronopotentiometric theory indicates that the diffusion coefficient of the nickel ions through the lattice can be calculated if the stoichiometry of the reactions and the concentration of the electroactive species are known. From the listed density of Ni_3S_2 [19] and the stoichiometry calculated here the mean values of D, the diffusion coefficient, have been calculated to the ends of each stage of reaction (Table 2) for the present work and for that of Kato and Oki [17]. In addition the activation energy of the diffusion process has been calculated from these two investigations (Table 3).

3.2. *Nickel matte*

The anodic reactions of polished specimens of nickel matte were examined at 40, 50 and 60° C

Table 2. Diffusion coefficients and activation energy of nickel ions in Ni_3S_2

	D (m^2 s^{-1})			
Temperature (°C)	*Stage 1*	*Inflection*	*Stages (1 + 2)*	*Stages (1 + 2 + 3)*
(1) Present investigation				
50	2.98×10^{-12}	2.97×10^{-12}	3.00×10^{-12}	2.98×10^{-12}
(2) Kato and Oki [17]				
40			2.32×10^{-12}	2.36×10^{-12}
Activation energies (J mole^{-1})			10 200	11 200

Table 3. The anodic treatment of nickel matte 100 g, H_2SO_4 dm^{-3}. Average values of $i_o t^{1/2}$ Am^{-2} $s^{1/2}$

Temperature (°C)	Current density (Am^{-2})	$i_o t^{1/2}$ Prewave	Stage 1	Inflection	Stages (1 + 2)	Stages (1 + 2 + 3)
40	250	9951	12646	16130	17498	–
	500	10794	11445	15211	17341	40942
	1000	12301	10733	13889	16068	26810
	1500	12650	11819	–	15756	23557
	2000	12285	11251	12961	14432	20726
50	250	13829	14131	21881	24186	–
	500	11084	11873	18884	20978	–
	1000	11467	11702	18393	21278	31578
	1500	12302	10569	15934	18630	26380
	2000	11776	10849	14235	16099	23807
60	500	13807	11710	25150	28309	–
	1000	15569	10003	20267	23780	37686
	1500	15909	10521	19409	22622	32312
	2000	15498	10126	17405	20391	29696
	2500	17294	10426	17509	21102	29623

in a solution of 100 g H_2SO_4 dm^{-3}, at current densities of 250 and 2500 Am^{-2}.

The shape of the potential–time relationship is shown in Fig. 3. By comparison with Fig. 1 it can be seen that there is an additional first stage, which in this paper will be referred to as the 'prewave stage'.

The low potential in the prewave range corresponds to dissolution of the metallic nickel phase in the matte. When the rate of reaction of this phase was insufficient to maintain the imposed current alone the potential rose to a value where the Ni_3S_2 phase reacted (Fig. 3, point X) in a manner identical to the stages previously noted with synthetic Ni_3S_2. Nickel ions were liberated during Stages 1 and 2, and sulphur was found to be present during Stage 3. In Stage 4, oxygen was evolved in addition to the electrochemical dissolution of the two matte phases.

The values of $i_o t^{1/2}$ have been calculated for all the stages, but for Stages 1, 2 and 3, $t = 0$ is taken as the end of the prewave stage. This assumption is essential as the treatment involves the reaction of two separate phases within a single electrode.

The average values of $i_o t^{1/2}$ for 40, 50 and 60° C are listed in Table 3. It is apparent that

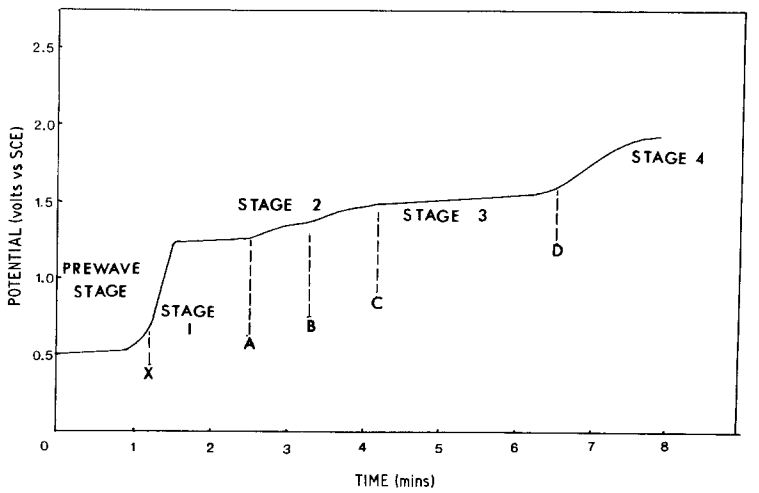

Fig. 3. Potential–time relationship for nickel matte anodically treated in 100 g H_2SO_4 dm^{-3}. 1500 Am^{-2}, 50° C.

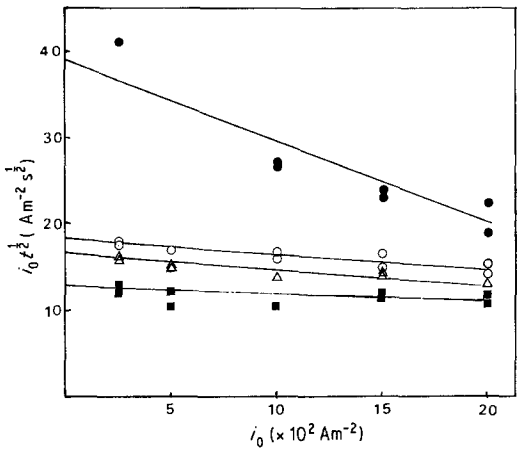

Fig. 4. $i_0 t^{1/2}$ versus i_0 relationship for nickel matte treatment. 40° C, 100 g H_2SO_4 dm^{-3}. • Stage 3; ○ Stage 2; △ inflection; ■ Stage 1.

$i_0 t^{1/2}$ is not constant for any stage. The results can be quantitatively treated by either: (a) classical chronopotentiometric theory, or; (b) adaption of the solid state diffusion theory previously adopted.

(a) Chronopotentiometric theory indicates that if the electrochemical reaction is preceded by a rate-determining chemical reaction the value of $i_0 t^{1/2}$ will decrease with an increase of i_0 [20]. In a previous paper [13] it was shown that at $i_0 = 0$ and where $i_0 \to \infty$ the equations reduce to those for diffusion control and, therefore, the stoichiometry of the reaction may be found. In addition, extrapolation of the plot of $i_0 t^{1/2}$ versus i_0 to $i_0 = 0$ will give the value of $i_0 t^{1/2}$ for diffusion control. This plot has been drawn for treatment at 40° C (Fig. 4) and it can be seen that the values of $i_0 t^{1/2}$ can be extrapolated to $i_0 = 0$ and a limiting value is attained where $i_0 \to \infty$. The values of $i_0 t^{1/2}$ for diffusion control, i.e. at $i_0 = 0$, are listed (Table 4a) in addition to the activation energy of the reaction. From the values of $i_0 t^{1/2}$ at $i_0 = 0$ and $i_0 \to \infty$, the values of x ($Ni_{3-x}S_2$) have also been calculated (Table 5).

(b) As indicated in the previous reanalysis of the work of Kato and Oki, the plot of $i_0 t^{1/2}$ versus $t^{1/2}$ will extrapolate to the value of $i_0 t^{1/2}$ for diffusion control at $t^{1/2} = 0$ (Fig. 5). From this plot, it appears possible that $i_0 t^{1/2}$ may tend towards a limit at large values of $t^{1/2}$. This has not been predicted by the theory presented. The values of $i_0 t^{1/2}$ at $t^{1/2} = 0$ are listed and the corresponding activation energies (Table 4a, b) and the values of x in the intermediate phases ($Ni_{3-x}S_2$) have also been calculated (Table 5) for $t^{1/2} = 0$.

Comparison of the values of $i_0 t^{1/2}$, the activation energy, and x by the above two methods with the corresponding values previously calculated for synthetic Ni_3S_2 (Tables 1, 2, 4a, b)

Table 4a. Nickel matte electrolysis. Calculated values of $i_0 t^{1/2}$ for diffusion control

Temperature (°C)	*Stage 1*	*Inflection*	*Stages (1 + 2)*	*Stages (1 + 2 + 3)*
A. Chronopotentiometric theory. $i_0 t^{1/2}$ at $i_0 = 0$				
40	13002	16791	18128	38822
50	13583	22061	25220	38030
60	11649	26580	30003	45216
B. Solid-state diffusion theory. $i_0 t^{1/2}$ at $t^{1/2} = 0$				
40	10964	12538	13281	17264
50	10397	11349	12776	18738
60	10467	15444	19663	12252

Table 4b. Nickel matte electrolysis. Activation energy (J $mole^{-1}$)

	Stages (1 + 2 + 3)
A. Chronopotentiometric theory	13100
B. Solid-state diffusion theory	33100

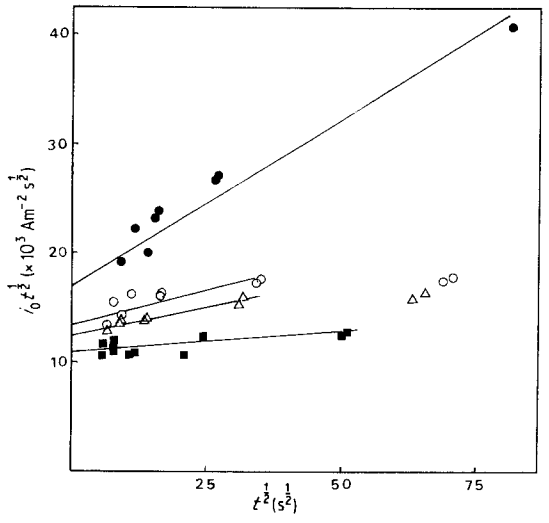

Fig. 5. $i_o t^{1/2}$ versus $t^{1/2}$ relationship for nickel matte treatment. 40° C, 100 g H_2SO_4 dm^{-3}. • Stage 3; ○ Stage 2; △ inflection; ▪ Stage 1.

Table 5. Nickel matte electrolysis. Calculated values of x ($Ni_{3-x}S_2$)

Temperature (°C)	*Stage 1*	*Inflection*	*Stages (1 + 2)*
(1) Chronopotentiometric theory			
(A) $i_o = 0$			
40	1.00	1.26	1.40
50	1.07	1.74	1.99
60	0.77	1.76	1.99
(B) $i_o \to \infty$			
40	1.56	1.76	2.05
50	1.35	1.80	2.02
60	1.04	1.77	2.10
(2) Solid-state diffusion theory			
$t^{1/2} = 0$			
40	1.91	2.18	2.31
50	1.66	1.82	2.05
60	1.24	1.95	2.34

indicates a slightly better agreement with the analysis using classic chronopotentiometric theory.

No attempt has been made at the present time to analyse the dissolution of the metallic phase in the prewave stage of the reaction sequence because of insufficient information on the composition of this phase and the changes the phase undergoes during anodic treatment. It is apparent, however, (Table 3) that this may also involve solid-state diffusion [21] with possible chemical effects of the solution.

3.3. *β-NiS*

The reactions of synthetic β-NiS were investigated at 50° C at 250–2000 Am^{-2} in 100 g H_2SO_4 dm^{-3} and at 3800–5500 Am^{-2} in a solution of (60 g dm^{-3} Ni^{2+} + 100 g dm^{-3} NaCl + 20 g dm^{-3} H_3BO_3 + 102 g dm^{-3} H_2SO_4). The latter solution corresponds to the composition of the electrolyte used in the INCO matte electrolysis process [3].

The shape of the potential–time plot in all cases was as indicated in Fig. 6. There were four stages in the reaction sequence: during Stage 1 an almost constant potential was maintained, while in Stage 2 the potential increased much more rapidly with time. After this second stage the potential again increased at a much reduced rate during Stage 3. In the final stage, Stage 4, there was a rapid transition to a high, varying potential at which oxygen was observed to be evolving.

Solution and solid-state analyses indicated that

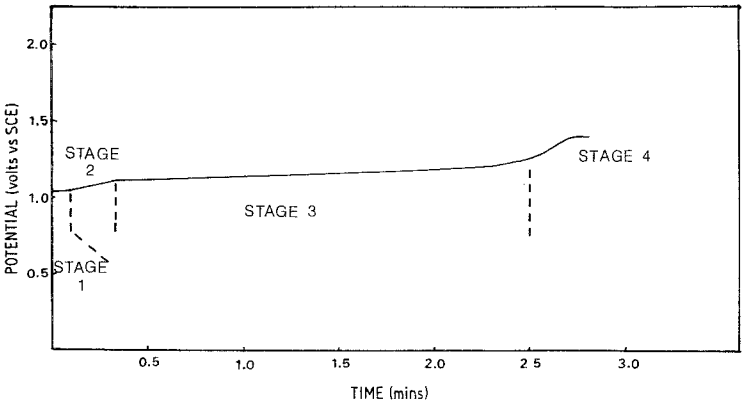

Fig. 6. Potential–time relationship for β-NiS anodically treated at 100 g H_2SO_4 dm^{-3}, 500 Am^{-2}, 50° C.

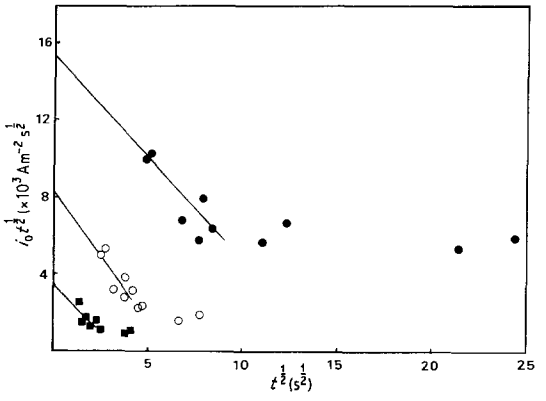

Fig. 7. $i_o t^{1/2}$ versus $t^{1/2}$ relationship for β-NiS treatment. 50° C, 100 g H_2SO_4 dm^{-3}. • Stage 3; ○ Stage 2; ▪ Stage 1.

nickel went into the solution at all stages, but sulphur was found to be present only in Stages 3 and 4. No phases other than sulphur and β-NiS could be detected in any product by X-ray diffraction analysis, but the results of the potential changes and the sulphur detection suggest that during Stages 1 and 2 the reactions occurring are:

$$NiS \rightarrow Ni_{1-x}S + xNi^{2+} + 2xe^- \quad (9)$$

$$Ni_{1-x}S \rightarrow (1-x)Ni^{2+} + S^0 + 2(1-x)e^-. \quad (10)$$

The average values of $i_o t^{1/2}$ for the anodic treatments in the two solutions at 50° C are represented in graphical form in Figs 7 and 8.

Analysis of the data for the anodic treatments in H_2SO_4 solution by classic chronopotentiometric analysis, with $i_o t^{1/2}$ increasing with i_o, would indicate possible adsorption effects [21], but by combination of the solid-state diffusion analysis now employed with Equations 9 and 10, then:

$$\frac{n_2}{n_1} = \frac{(t_1 + t_2)^{1/2} - t_1^{1/2}}{t_1^{1/2}} = \frac{1-x}{x} \quad (11)$$

where t is the value found from $i_o t^{1/2}$ extrapolated to $t^{1/2} = 0$. n_1 and t_1 refer to the preferential nickel dissolution of Stages 1 and 2; and n_2 and t_2 correspond to Stage 3, where the resulting nickel deficient sulphide decomposes, liberating sulphur.

Figs 7 and 8 illustrate the extrapolation of $i_o t^{1/2}$ versus $t^{1/2}$. Despite the great differences in the general forms of the $i_o t^{1/2}$ versus $t^{1/2}$ plots it is apparent that the values of $i_o t^{1/2}$ at $t^{1/2} = 0$ are equivalent for each stage within the margins of error of the extrapolations ($\simeq$ 20% for Fig. 7, $\simeq$ 50% for Fig. 8).

From the results in H_2SO_4 solution the values of x in the intermediate phases, $Ni_{1-x}S$, have been calculated. The intermediates indicated by the analysis, $Ni_{1.6}S$ and NiS_2, are equivalent to those previously found during anodic treatment of Ni_3S_2 and nickel matte, $Ni_{1.5}S_2$ and NiS_2. The latter values are considered to be more reliable because of the greater precision of the results and analyses. The $Ni_{1.2}S_2$ phase was not indicated in the treatment of β-NiS, but the potential changes during the treatment of millerite could not be followed with sufficient precision to detect whether there was a slight inflection present that would indicate this further intermediate.

Although previous investigations of the anodic treatment of millerite have not suggested the presence of nickel deficient phases, as in the treatment of heazlewoodite, this is apparently due to the reliance on the determination of millerite by X-ray diffraction, although recent work [22] on

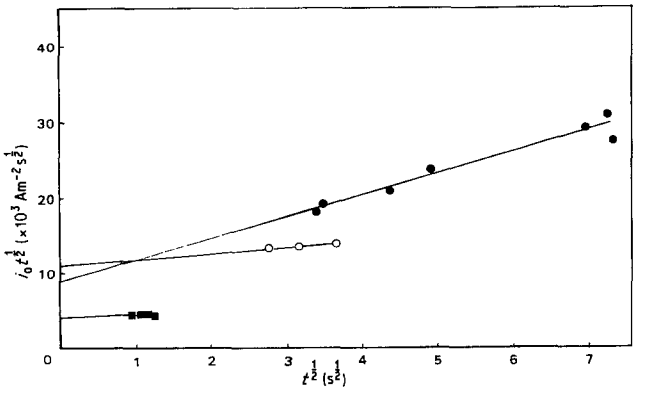

Fig. 8. $i_o t^{1/2}$ versus $t^{1/2}$ relationship for β-NiS treatment at 50° C in chloride sulphate electrolyte. • Stage 3; ○ Stage 2; ▪ Stage 1.

solid phase analyses indicates the possible presence of nickel deficient phases.

The corresponding values of the diffusion coefficient of the nickel ion in the crystal have also been calculated using a published value [23] for the density of β-NiS. The diffusion coefficients (e.g. 2.36×10^{-12} m^2 s^{-1} for the total reaction) are in reasonable agreement with previous analyses of the anodic treatment of Ni_3S_2.

From Fig. 7, it can be seen that the values of $i_o t^{1/2}$ approach limiting values at high $t^{1/2}$ values. These limiting values are not in the same proportions as the values at $t^{1/2} = 0$ (i.e. using the previous analysis the values of x are calculated to be 0.16 and 0.3).

4. Discussion

The present investigation has indicated the presence of intermediates in the electroleaching of nickel sulphides that have not usually been reported during hydrometallurgical treatment. However, from a phase diagram of the Ni–S system a number of these intermediates could have been anticipated [24]. From this, it is predicted that the removal of nickel from Ni_3S_2 by leaching should proceed through the following series of phases:

$$Ni_3S_2 \rightarrow Ni_7S_6 \rightarrow NiS \rightarrow Ni_3S_4 \rightarrow NiS_2 .$$

This is in agreement with the present findings of $Ni_{1.5}S_2$ and NiS_2 in the leaching sequence, although there was no indication of the compound Ni_7S_6. Re-examination of the rest potential–composition measurements in the Ni–S system by Ivanov [25] indicate a compound of composition Ni_6S_5, although it is stated that this is a metastable phase.

The difficulty of determining the slight increases in potential during electroleaching that indicate the presence of intermediates has been referred to in previous papers [13, 14]. It appears that rest potential–composition measurements for the range $Ni_3S_2 \rightarrow Ni_{0.2}S_2$ would provide a relatively simple way of determining which compounds are stable in this system (cf. Koch and McIntyre [26] for an excellent application of this method to the Cu–S system).

The value of the solid-state diffusion coefficient of nickel found in the present experiments appears to be relatively high. However, this has been explained by Wagner [27] as being due to the fact that it is the interdiffusion coefficient rather than the self-diffusion coefficient that is being measured in the type of experiment now performed.

Acknowledgements

The authors wish to thank the Natural Science and Engineering Research Council of Canada for financial support of this research. Appreciation is also expressed to Professor W. M. Williams for making available facilities to perform this work. Particular gratitude is due to Mr H. Larsson who provided valuable help in many aspects of the project.

References

[1] M. Loshkarev, O. Esin and G. Lapp, *Zhur. Priklad. Khim.* **18** (1945) 294.
[2] L. S. Renzoni, R. C. McQuire and M. V. Baker, *J Metals* **10** (1965) 38.
[3] W. W. Spence and W. R. Cooke, *Trans. Can. Min. Met.* **67** (1967) 257.
[4] D. A. D. Boateng and C. R. Phillips, *Min. Sci. Eng.* **10** (1978) 155.
[5] A. L. Rotinyan, *Tsvetnye. Metall.* **32** (1954) 88.
[6] D. M. Chizhikov, *et al. Izv. Akad. Nauk. SSR* (1962) *Chemical Abstracts* **58** (1963) 1128h.
[7] I. S. Ivanov and V. L. Kheifets, *Tr. Proekt. Nauch. Issed Inst 'Gipronikel' (Gos. Inst. Proekt, Predpr Nickelevai Prom.)* **38** (1968) 71.
[8] I. S. Ivanov, *Zh. Pricklad Khim* **41** (1968) 1017.
[9] F. Habashi, *Min. Sci. Eng.* **3** (1971) 3.
[10] L. S. Sinev, N. S. Shchetinin and Y. G. Brodynskii, *Shur. Fiz. Kim.* **48** (1974) 1194.
[11] R. G. Bautista and D. S. Flett, Warren Spring Laboratory Report No. Lr 226 (ME) (1976) Stevenage, England.
[12] J. A. King, PhD thesis, University of London (1966).
[13] D. C. Price and J. P. Chilton, *Hydromet.* **7** (1981) 117.
[14] D. C. Price, *Met. Trans.* **12B** (1981) 231.
[15] H. J. S. Sand, *Phil. Mag.* **1** (1901) 45.
[16] T. Berzins and P. Delahay, *J. Amer. Chem. Soc.* **75** (1953) 4205.
[17] T. Kato and T. Oki, *Nippon Kinzoku Gakkaishi* **37** (1973) 1338.
[18] C. DeRantny and R. Breckpot, *Bull. Soc. Chem. Belges* **78** (1969) 503.
[19] ASTM, X-ray Diffraction Index, 8–126.
[20] P. Delahay and T. Berzins, *J. Amer. Chem. Soc.* **75** (1953) 2488.
[21] P. Delahay, 'New Instrumental Methods in Electrochemistry', Interscience Publishers, New York, (1954).
[22] E. Ghali, A. Maruejauls and D. Deroo, *J. Appl. Electrochem.* **10** (1980) 709.

[23] ASTM, X-ray Diffraction Index, 12–41.
[24] 'Gemlins Handbuch, Syst. 60, B(2)', Springer-Verlag, Berlin (1960) p. 627.
[25] I. S. Ivanov, *Zh. Prikl. Khim.* **41** (1968) 1017.
[26] D. F. A. Koch and R. J. McIntyre, *J. Electroanal. Chem.* **71** (1976) 285.
[27] C. Wagner, *Z. Chem. Phys.* **21** (1953) 1819.